Indirect dark matter search with the ANTARES neutrino telescope

Guillaume Lambard[*][†]

IFIC - Instituto de Física Corpuscular - Edificio Institutos de Investigación, Apartado de Correos 22085 E-46071 Valencia, Spain
E-mail: `lambard@ific.uv.es`

Using the data recorded by the ANTARES neutrino telescope during 2007 and 2008, a search for high energy neutrinos coming from the direction of the Sun has been performed. The neutrino selection criteria have been chosen so as to maximize the rejection of the atmospheric background with respect to possible signals produced by the self-annihilation of weakly interactive massive particles accumulated in the centre of the Sun. After data unblinding, the number of neutrinos observed was found to be compatible with background expectations. The results obtained were compared to the fluxes predicted by the Constrained Minimal Supersymmetric Standard Model, and 90% upper limits for this model were obtained. Our limits are competitive with those obtained by other neutrino telescopes such as IceCube and SuperKamiokande, which give ANTARES limits for the spin-dependent WIMP-proton cross-section that are more stringent than those obtained by direct search experiments.

---

[*]Speaker.

[†]on behalf of the ANTARES collaboration

1. Introduction

There is compelling evidence that 83% of the matter in the Universe is in the form of non-baryonic and non-relativistic matter that does interact weakly with the ordinary matter, the so-called dark matter. Much of this evidence comes from its gravitational effects on the motion of galaxies, clusters of galaxies and from the large scale structure of the Universe. The existence of dark matter is a key component of our present standard cosmological model, and results from the study of the CMB anisotropies and gravitational lensing in galaxy clusters further support its existence (for a review of the evidence, candidates and constraints, see [1] and [2]).

One of the most favoured hypothesis is that dark matter is made of weakly interacting massive particles (WIMPs) that are embedded in the visible, baryonic part of the galaxies and surround them in the form of a halo. There are a variety of candidates for WIMPs, among which those provided by theories based on supersymmetry (SUSY) or universal extra dimensions (UED) attract a great deal of interest. In some classes of SUSY, the lightest particle is stable due to the conservation of R-parity that forbid its decay to standard particles, making it a good candidate as a dark matter WIMP.

In addition to its gravitational effects, the search for evidence of the existence of WIMPs is at present performed, on the one hand, by looking for the recoiling products of the elastic scattering of dark matter particles off normal baryonic matter in suitable detectors, the so-called direct searches, and on the other hand, indirectly by the observation of the final products of the possible annihilation of WIMPs that have accumulated in astrophysical objects. WIMPs can scatter elastically in the Sun or the Earth and become trapped in their gravitational potential wells, accumulating in sizeable numbers over the age of the solar system, therefore a very wide region in the Galaxy must have contributed, reducing the dependence on the detailed structure of the dark matter halo. The WIMPs proposed by SUSY are Majorana fermions that can self-annihilate, giving rise to standard particles. Neutrinos will be at the end of the decay chain of the products of the WIMP self-annihilation, they can escape these astrophysical objects and be detected by neutrino telescopes on the Earth.

In this paper, the indirect search for dark matter looking for high energy neutrinos coming from the Sun using the data recorded by the ANTARES neutrino telescope in 2007 and 2008 is reported. The number of neutrinos observed is compared to the neutrino fluxes predicted by the Constrained Minimal Supersymmetric Standard Model (CMSSM) [3], a minimal supersymmetric extension of the Standard Model with supersymmetry-breaking scalar and gaugino masses constrained to be universal at the GUT scale.

The layout of the paper is as follows. In Section 2, the main features of the ANTARES neutrino telescope and the reconstruction algorithm used in this work are reviewed. In Section 3, the Monte Carlo simulations of the signal, expected from the investigated WIMP models, and the background, expected from atmospheric muons and neutrinos, are described. In Section 4, the method used to optimise the criteria to select the sample of neutrino events and reduce the background following a blind data strategy is presented. Finally, the results obtained are discussed in Section 5, where limits on the models investigated are imposed from the absence of a dark matter signal.

2. The ANTARES neutrino telescope

ANTARES is the first undersea neutrino telescope and the largest of its kind in the Northern Hemisphere [4]. It is located at 2475 m depth in the Mediterranean Sea, 40 km offshore from Toulon (France) at 42°48' N and 6°10' E.

The telescope consists of 12 mooring detection lines made up of 25 storeys each. The standard storey is composed of a local control module that contains the front-end and slow-control electronics and three optical modules (OMs) that house a 10-inch photomultiplier. The OMs are looking 45° downwards in order to optimise their acceptance to upgoing light and to avoid the effect of sedimentation and biofouling. The length of the lines is 450 m and the horizontal distance between neighbouring lines is 60-75 m. The absolute time accuracy is ensured at the millisecond level by the UTC time provided by the GPS system connected to the clock system of the detector. The relative time between the elements of the detector is achieved by calibration of the lines in the laboratory with short light pulses, by the use of a 25 MHz clock system and by the operation of a series of optical beacons distributed along the lines that emit short light pulses through the water. A relative timing of the order of one nanosecond is reached. Additional information on the detector can be found in reference [4].

Neutrinos are detected through the products of their interaction with the matter inside or close to the detector. In the channel of neutrino observation used in this work, a high energy neutrino interacts in the rock below the detector producing a relativistic muon that can travel hundreds of meters and cross the detector or pass nearby. This muon induces Cherenkov light when travelling through the water, which is detected by the OMs. From the time and position information of the hits in the OMs, the direction of the muon – which at high energy is essentially that of the neutrino – can be reconstructed.

Data-taking started in 2007 when only 5 lines of the detector where installed. The full detector was connected in May 2008 and has been operating ever since, except for some periods in which repair and maintenance operations have taken place. For this work the data taken during 2007 and 2008 has been used. Results of other searches using this data-taking period can be found elsewhere [5, 6, 7].

The reconstruction of the track from the position and time of the hits of the Cherenkov photons in the OMs is a key ingredient of the physics analysis. In this work, a dedicated fast algorithm to reconstruct the muon track is used [8]. The algorithm is based on the minimization of a χ^2-like quality parameter, Q, that uses the differences of the expected and actual times of the detected photons corrected by the effect of light absorption in water.

Monte Carlo simulations indicate that selecting tracks with a quality parameter per degree of freedom of the fit smaller than 1.4 results in a purity of 90% for upward reconstructed multi-line atmospheric neutrinos, the contamination being misreconstructed downgoing atmospheric muon events, with an angular resolution of about few degrees at energies of tens of GeV, driven at $\sim 40\%$ by the kinematic of the neutrinos in low energy regime.

3. Signal and background simulation

The number of muon neutrinos as a function of their energy arriving at the Earth's surface

from the Sun's core, dN_ν/dE_ν, is computed using the software package WimpSim [9]. The usual self-annihilation channels ($q\bar{q}$, $l\bar{l}$, WW, ZZ, Higgs doublets $\phi\phi^*$ and $\nu\bar{\nu}$) were simulated for 17 different WIMP masses from 10 GeV to 10 TeV. Oscillations between the three neutrino flavours both in the Sun and during their flight to Earth as well as ν absorption and τ lepton regeneration in the Sun are taken into account.

For the CMSSM, three main self-annihilation channels were chosen for the lightest neutralino, $\tilde{\chi}_1^0$, namely: a soft neutrino channel, $\tilde{\chi}_1^0\tilde{\chi}_1^0 \to b\bar{b}$, and two hard neutrino channels, $\tilde{\chi}_1^0\tilde{\chi}_1^0 \to W^+W^-$ and $\tilde{\chi}_1^0\tilde{\chi}_1^0 \to \tau^+\tau^-$. Since which of these three channels is dominant depends on the region of the CMSSM parameter space being analysed [10], a 100% branching ratio was assumed for all of them in order to explore them on an equal footing.

The main backgrounds for this search are muons and neutrinos produced in the interaction of cosmic rays with the atmosphere. Downgoing atmospheric muons dominate the trigger rate, which ranges from 3 to10 Hz depending on the exact trigger conditions. They are simulated using Corsika [11]. Upgoing atmospheric neutrinos, which are recorded at a rate of ~1 mHz (about four per day) [4], are simulated according to the parametrisation of the atmospheric ν_μ flux from [12] in the energy range from 10 GeV to 10 PeV.

The Cherenkov light produced in the vicinity of the detector is propagated taking into account light absorption and scattering in sea water. The angular acceptance, quantum efficiency and other characteristics of the PMTs are taken from [13] and the overall geometry corresponded to the layout of the ANTARES detector [4] according to the data taking periods (from 5 to 12 line configurations).

4. Optimisation of the event selection criteria

The data set used in this analysis comprises a total of $2,693$ runs recorded between the 27th of January 2007 and the 31st of December 2008, corresponding to a total livetime of ~294.6 days. The detector consisted of 5 lines for most of 2007 and of 9, 10 and 12 lines for 2008.

Only upgoing events are kept in the analysis. The muon tracks are required to have $\cos\theta <$ 0.9998 in order to exclude those for which the fit stopped at the boundary. The fit is required to use a number of hits greater than five in at least two lines in order to ensure a non-degenerate 5-parameter fit with a proper reconstruction of the azimuth angle.

The UTC time of the events is uniformly randomised on the period of the data taking in order to estimate the background in the Sun's direction from the data itself. The local coordinates (θ, ϕ) are kept so as to preserve the detector geometry in the optimisation of the selection criteria. This procedure provides a means to follow a *data blinding* strategy while using all the relevant information on the detector's performance.

The values used in the event selection criteria for the quality parameter, Q, and for the aperture of the search cone in the Sun's direction, Ψ, are optimised following the model rejection factor (MRF) technique [14]. For each WIMP mass and each annihilation channel, the values of Q and Ψ used are those that minimized the MRF as defined by:

$$MRF = \frac{\bar{\mu}^{90\%}}{\sum_i A_{eff}^i(M_{\text{WIMP}}) \times T_{eff}^i} ,$$ (4.1)

where the index i denotes the different periods in the detector infrastructure (5, 9, 10 and 12 detection lines), $\bar{\mu}^{90\%}$ is the average upper limit at 90% confidence level (CL) computed from the time-scrambled data set and using a Poisson distribution in the Feldman-Cousins approach [15]; T_{eff}^{i} is the livetime for each detector configuration in 2007-2008, namely: $\sim$134.6, $\sim$38, $\sim$39 and $\sim$83 days for 5, 9, 10 and 12 lines respectively. The effective area averaged over the neutrino energy, $A_{eff}(M_{\text{WIMP}})^{i}$, is defined as (the index i is implied):

$$A_{eff}(M_{\text{WIMP}}) = \sum_{\nu,\bar{\nu}} \left(\frac{\int_{E_{\nu}^{th}}^{M_{\text{WIMP}}} A_{eff}(E_{\nu,\bar{\nu}}) \frac{dN_{\nu,\bar{\nu}}}{dE_{\nu,\bar{\nu}}} dE_{\nu,\bar{\nu}}}{\int_{0}^{M_{\text{WIMP}}} \frac{dN_{\nu}}{dE_{\nu}} dE_{\nu} + \frac{dN_{\bar{\nu}}}{dE_{\bar{\nu}}} dE_{\bar{\nu}}} \right) , \tag{4.2}$$

where $E_{\nu}^{th} = 10$ GeV is the energy threshold for neutrino detection in ANTARES, M_{WIMP} is the WIMP mass, $dN_{\nu,\bar{\nu}}/dE_{\nu,\bar{\nu}}$ is the energy spectrum of the neutrinos or the anti-neutrinos at the surface of the Earth for the three channels of interest in this analysis, and $A_{eff}(E_{\nu,\bar{\nu}})$ is the effective area of ANTARES as a function of the neutrino or anti-neutrino energy. Due to their different cross-sections these two effective areas are slightly different and therefore are studied separately.

5. Results and discussion

Once the optimised values of Q and Ψ were obtained using the time-scrambled data, the data sample is unblinded. Figure 1 shows the distribution of the spatial angle between the tracks of the events and the Sun's direction obtained after applying the basic selection criteria on the zenith angle and the minimum number of hits and lines. A total of 27 events were found within a 20 degrees spatial angle and no excess in the Sun's direction above the scrambled background are observed.

Using the values for the cuts obtained in the optimisation procedure, limits on the $\nu_{\mu} + \bar{\nu}_{\mu}$ flux, $\phi_{\nu_{\mu}+\bar{\nu}_{\mu}}$, can be extracted from the data according to:
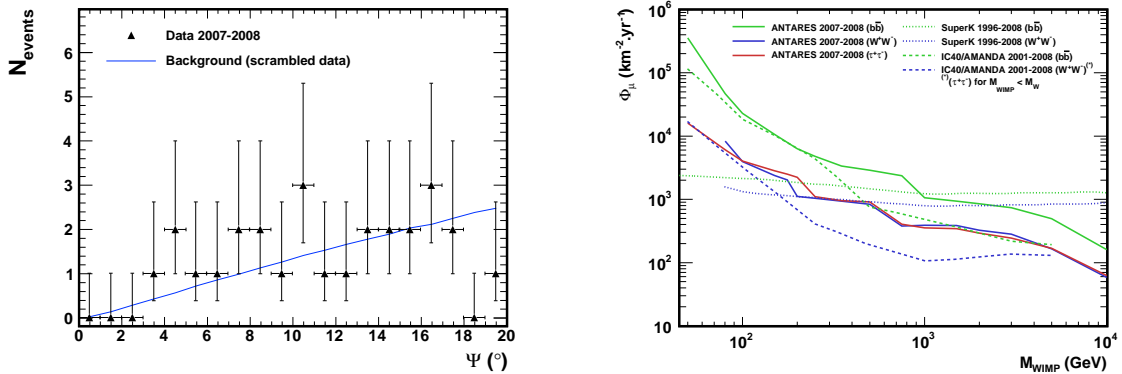

Figure 1: Left: Distribution of the spatial angle $\Psi \in [0^{o}, 20^{o}]$ of the event tracks with respect to the Sun's direction for the expected background computed from the time-scrambled data (solid blue line) compared to the data after the basic selection criteria (black triangles) . A 1σ Poisson uncertainty is shown for each data point (black cross). **Right:** 90% CL upper limit on the muon flux as a function of the WIMP mass in the range $M_{\text{WIMP}} \in [50$ GeV;10 TeV] for the three channels $b\bar{b}$ (green), $W^{+}W^{-}$ (blue) and $\tau^{+}\tau^{-}$ (red, ANTARES only). The results from SuperKamiokande $1996 - 2008$ [17] (dotted lines) and IceCube-40 plus AMANDA 2001-2008 [18] (dashed lines) are also shown.

$$\phi_{\nu_\mu + \bar{\nu}_\mu} = \frac{\mu^{90\%}}{\sum_i A^i_{eff}(M_{\text{WIMP}}) \times T^i_{eff}} ,$$ (5.1)

where $\mu^{90\%}$ is the upper limit at 90% CL on the number of observed events and the rest of variables have the same meaning as in Eq. 4.1.

The corresponding limits for muons are calculated using a conversion factor between the neutrino and the muon fluxes ($\phi_\mu = \Gamma_{\nu \to \mu} \times \phi_{\nu_\mu + \bar{\nu}_\mu}$) computed using DarkSusy [16]. Figure 1 (on the right) shows the 90% CL muon flux limits ϕ_μ for the channels $b\bar{b}$, W^+W^- and $\tau^+\tau^-$. The latest results from SuperKamiokande [17] and IceCube-40 plus AMANDA [18] are also shown for comparison. Despite its smaller detector volume, the ANTARES limits both in the soft and hard channels are similar to those obtained by IceCube40 and AMANDA in the mass range $M_{\text{WIMP}} \in [50;100]$ GeV. In this mass range most of the sensitivity of the South Pole telescopes comes from AMANDA-II, whose effective area and energy threshold were similar to those of ANTARES in its 12-line configuration. Compared to the limits set by SuperKamiokande, those of ANTARES are more stringent in the high mass region $M_{\text{WIMP}} > 150$ GeV.

Systematic uncertainties have been taken into account and included in the evaluation of the limits using the approach of reference [23] by means of the `Pole` software. The total systematic uncertainty on the detector efficiency is around 20% and comes mainly from the efficiency and time resolution uncertainties of the OMs, the total angular resolution and the absolute pointing accuracy. This uncertainty translates into an increase of the upper limit between 3% and 6% depending on the WIMP mass.
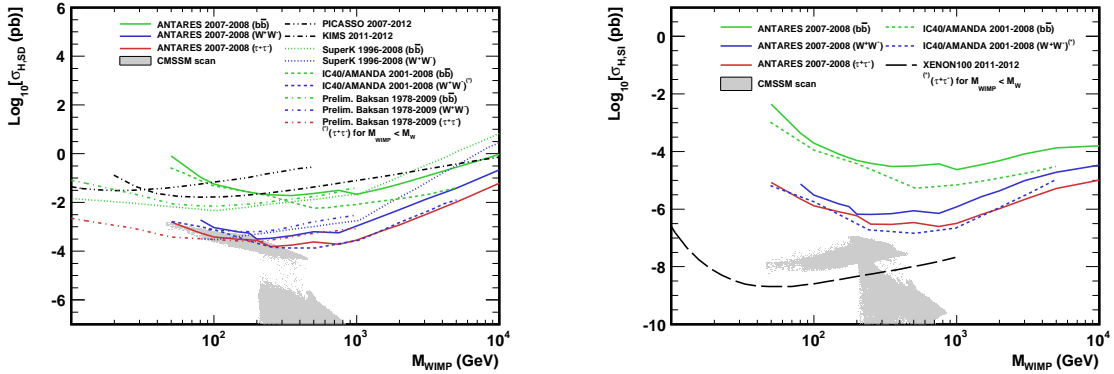

Figure 2: 90% CL upper limits on the SD and SI WIMP-proton cross-sections (left and right hand respectively) as a function of the WIMP mass in the range $M_{\text{WIMP}} \in [50 \text{ GeV};10 \text{ TeV}]$, for the three channels: $b\bar{b}$ (green), W^+W^- (blue) and $\tau^+\tau^-$ (red), for ANTARES (solid line) compared to the results of other indirect search experiments: SuperKamiokande $1996 - 2008$ [17] (dotted lines) ,IceCube-40 plus AMANDA 2001-2008 [18] (dashed lines) and Baksan $1978 - 2009$ [19] (colored dot-dashed line) and the result of the most stringent direct search experiments (black): PICASSO $2007 - 2012$ [21] (two-dots-dashed line), KIMS $2011 - 2012$ [20] (black dot-dashed line) and XENON100 $2011 - 2012$ [22] (dashed line). For a comparison to the theoretical expectations, grid scans corresponding to the CMSSM model have been added.

Assuming equilibrium between the WIMP capture and self-annihilation rates in the Sun, the

limits on the spin-dependent (SD) and the spin-independent (SI) WIMP-proton scattering cross-sections can be obtained for the case in which one or the other is dominant.

A conservative approach to the dark matter local halo was considered assuming a gravitational effect of Jupiter on the Sun's capture rate, which reduces about 13% (87%) the SD capture and about 1% (12%) the SI capture for 1(10) TeV WIMPs. A local dark matter density of about 0.3 GeV.cm^{-3} was assumed. No additional dark matter disk that could enhance the local dark matter density was considered (see [24] for a discussion).

The 90% CL limits for the SD and SI WIMP-proton cross-sections extracted from the channels $b\bar{b}$, W^+W^- and $\tau^+\tau^-$ are presented in Figure 2. The latest results from SuperKamiokande, IceCube-40+AMANDA and Baksan together with the latest and the most stringent limits from the direct search experiments PICASSO, KIMS and XENON100 are also shown. The allowed parameter space from CMSSM model according to the results from an adaptive grid scan performed with DarkSUSY 5.0.6 [16] are also shown. For a proper comparison all the limits presented in Figure 2 are computed with a muon energy threshold at $E_\mu = 1$ GeV. For these figures, the shaded regions show a grid scan of the model parameter space taking into account the last limits for the Higgs boson mass from ATLAS and CMS merged together such as $M_H = 125 \pm 2 GeV$. A relatively large constraint on the neutralino relic density $0 < \Omega_{CDM}h^2 < 0.1232$ is used not to enclose the studied dark matter particle to only one possible nature.

The neutrino flux due to WIMP annihilation in the Sun is highly dependent on the capture rate of WIMPs in the core of the Sun, which in turn is dominated by the SD WIMP-proton cross-section. This makes these indirect searches better compared to direct search experiments such as KIMS and COUPP. This is not the case for the SI WIMP-proton cross-section, where the limits coming from direct search experiments such as CDMS and XENON100 are better thanks to their target materials. Therefore, there is a sort of complementarity between both types of searches.

Indirect Dark Matter search in the Sun with ANTARES　　　　　　　　Guillaume Lambard

References

[1] G. Bertone, D. Hooper, J. Silk, Phys.Rept., 2005, **405**: pp. 279-390.

[2] Particle Data Group, J. Phys. G **37**, 070521 (2010).
http://pdg.lbl.gov/2011/reviews/rpp2011-rev-dark-matter.pdf.

[3] J. Ellis, K.A. Olive, C. Savage, and V.C. Spanos, Phys. Rev. D **81**, 085004 (2010).

[4] M. Ageron et al., ANTARES Collaboration, Nucl. Inst. and Meth. in Phys. Res. A **656** (2011) 11-38
[astro-ph/1104.1607].

[5] J.A. Aguilar, ANTARES Collaboration, Phys. Lett, **B696** (2011) 16.

[6] S. Adrián-Martínez et al., ANTARES Collaboration, Ap. J. Letter **743** (2011) L14.

[7] S. Adrián-Martínez et al., ANTARES Collaboration, Astropart. Phys. **35** (2012) 634.

[8] J.A. Aguilar, ANTARES Collaboration, Astropart. Phys. **34** (2011) 652.

[9] J. Edsjö, http://www.physto.se/ edsjo/wimpsim/.

[10] S. Desai et al., Phys. Rev. D **70**, 083523 (2004).

[11] D. Heck et al., Report FZKA 6019 (1998), Forschungszentrum Karlsruhe; D. Heck and J. Knapp,
Report FZKA 6097 (1998), Forschungszentrum Karlsruhe.

[12] G. Barr et al., Phys. Rev. D **39** (1989) 3532; V. Agrawal et al., Phys. Rev. D **53** (1996) 1314.

[13] P. Amram et al., [ANTARES Collaboration], Nucl. Instrum. Meth. A **484** (2002) 369.

[14] G.C. Hill, K. Rawlins, Astropart. Phys., 2003, **19**: pp. 393-402.

[15] G.J. Feldman, R.D. Cousins, Phys. Rev., 1998, **D 57**: pp. 3873-3889.

[16] P. Gondolo et al., J. Cosm. and Astropart. Phys., JCAP07, 008 (2004).

[17] T. Tanaka et al., Astrophys. J. **742**, 78 (2011).

[18] R. Abbasi et al., Phys. Rev. D **85**, 042002 (2012).

[19] O. Suvorova et al., in proceedings of Dark Side of the Universe, PoS(DSU2012)042
[astro-ph/1211.2545].

[20] H. S. Lee et al., Phys. Rev. Lett. **108**, 181301 (2012) [astro-ph/1204.2646].

[21] S. Archambault et al., Phys. Lett. B **711** (2012) 153-161 [astro-ph/1202.1240].

[22] E. Aprile et al. [astro-ph/1207.5988].

[23] F. Tegenfeldt, J. Conrad A NIM A **539** (2005) 407-413; J. Conrad et al., Phys. Rev. D **67** (2003)
012002; J. Conrad (2006) [astro-ph/0612082v1].

[24] G. Wikström and J. Edsjö, J. Cosm. and Astropart. Phys., JCAP04, 009 (2009).